

Traditional MPs and Degradable MPs Differences in Arsenic Adsorption and Their Mechanisms

Artur Duchateau¹, Thomas Rager^{2,*}

¹ SABIC Technology Center at KAUST, 25 Unity Blvd, 23955 Thuwal, Saudi-Arabia

² Chimie Moléculaire, Macromoléculaire, Matériaux, ESPCI Paris, Université PSL, CNRS, 75005 Paris, France

*Corresponding author: T11206Rager@espci.psl.eu

Abstract. To investigate the differences and mechanisms in the adsorption behavior of As(V) between degradable MPs (PCL, PLA) and conventional non-degradable MPs (PE, PP), this study conducted batch adsorption experiments to compare the adsorption kinetics and thermodynamics of the two types of MPs under three particle sizes (100 μm , 150 μm , 200 μm). Isotherm modeling was conducted by applying the Langmuir and Freundlich theories to interpret the collected experimental results. The reaction dynamics were evaluated using first-order and second-order pseudo-kinetic approaches, complemented by structural and compositional analyses through FTIR spectroscopy and XRD patterns. The results showed that the specific surface area and total pore volume of degradable MPs were approximately 5 and 10 times higher than those of conventional MPs, respectively. The surfaces of degradable MPs were rich in oxygen-containing polar functional groups such as C=O and C-O-C, whereas conventional MPs were dominated by non-polar C-H groups. The adsorption capacity for As(V) followed the order: PLA-MPs (135.93 $\text{mg}\cdot\text{kg}^{-1}$) > PCL-MPs (98.94 $\text{mg}\cdot\text{kg}^{-1}$) > PE-MPs (87.18 $\text{mg}\cdot\text{kg}^{-1}$) > PP-MPs (79.12 $\text{mg}\cdot\text{kg}^{-1}$). The adsorption process of degradable MPs was better described by the pseudo-second-order kinetic model, indicating a dominant role of chemisorption. In contrast, conventional MPs exhibited comparable fitting degrees for both pseudo-first-order and pseudo-second-order models, suggesting that their adsorption was jointly controlled by physical interactions and weak chemical processes. The C=O and C-O-C groups in degradable MPs served as key sites for coordinative adsorption of As(V), while conventional MPs only participated in weak physical adsorption via C-H groups. Decreasing particle size enhanced the adsorption performance of all MPs, with this effect being particularly pronounced for conventional MPs, implying that their adsorption relies more heavily on specific surface area. The enhanced As(V) removal efficiency and accelerated sorption rates observed in degradable microplastics can be attributed to their porous architecture coupled with polar functional moieties present on the surface, thereby potentially serving as more efficient vectors for arsenic transport within environmental systems. This study provides a theoretical basis for scientifically assessing the composite pollution risks of the two types of microplastics and formulating differentiated environmental management strategies..

Keywords: Cellulose; Polyvinyl alcohol; Ionic gel; High-voltage window; Integrated flexible supercapacitors

Received on 15 March 2023, Accepted on 21 May 2023, Published on 28 June 2023

Copyright © 2023 Artur Duchateau and Thomas Rager licensed to JFMAE. This is an open access article distributed under the terms of the CC BY-NC-SA 4.0, which permits copying, redistributing, remixing, transformation, and building upon the material in any medium so long as the original work is properly cited.

1 Introduction

The advent of the "Plastic Age" has brought about unprecedented convenience to modern society, yet it has simultaneously precipitated a profound and persistent environmental crisis. Global plastic production has surged exponentially since the mid-20th century, exceeding 300 million tons annually and leading to the accumulation of vast quantities of plastic waste in natural ecosystems [1]. A significant fraction of this waste undergoes progressive fragmentation through mechanical abrasion, ultraviolet radiation, and biological activity, giving rise to microplastics (MPs)—plastic particles defined as being smaller than 5 mm in diameter [2]. These microscopic pollutants have transcended their original sources to become ubiquitous contaminants, detected from the deepest ocean trenches to remote mountain glaciers, and from urban soils to agricultural lands [3-8]. Their small size, large specific surface area, and persistent nature make them highly mobile in the environment and susceptible to ingestion by a wide range of organisms, thereby introducing them into food webs and posing insidious risks to ecological health and potentially human safety.

In agricultural landscapes, the proliferation of MPs is intricately linked to the widespread adoption of plastic film mulching, a technology that conserves soil moisture, suppresses weeds, and enhances crop yields. However, the environmental management of these films post-harvest remains a significant challenge. Recovery rates are often dismal, frequently below two-thirds, leaving substantial amounts of plastic residue to be tilled into the soil matrix [9-11]. Over time, these macroplastic fragments break down into secondary MPs, making agricultural soils a major long-term reservoir for these particles. Traditionally, agricultural mulching films have been fabricated utilizing robust, non-biodegradable polymeric materials—specifically polyethylene and polypropylene—engineered for extended service life yet resulting in environmental persistence spanning hundreds of years. Driven by escalating apprehensions regarding plastic-induced environmental contamination and deteriorating soil quality, biodegradable polymeric films have gained considerable attention as a viable sustainable substitute. These films are typically composed of polymers like polycaprolactone (PCL) and polylactide (PLA), which are designed to undergo microbial degradation into water, carbon dioxide, and biomass under specific environmental conditions. While this addresses the issue of visual persistence, the environmental fate and behavior of the degradation intermediates and the MPs generated from these biodegradable materials are far less understood than their conventional counterparts.

A critical dimension of MP pollution extends beyond their physical presence to their role as vectors for other hazardous contaminants. The inherently hydrophobic character of microplastic surfaces, frequently accompanied by electrostatic charges or surface functionalization, facilitates the sequestration of diverse co-existing contaminants, ranging from persistent organic pollutants and pharmaceutical residues to various heavy metal species, present in the ambient milieu. This adsorption can significantly alter the environmental fate, transport, and bioavailability of these "hitchhiking" contaminants. For example, microplastics can function as transport vectors, enabling the dissemination of surface-bound toxicants over extensive distances into previously uncontaminated ecosystems or subsurface soil horizons. Alternatively, they may concentrate pollutants, creating localized hotspots of toxicity. While a growing body of research has begun to elucidate the interactions between traditional, non-degradable MPs (e.g., PE, PP, polystyrene (PS)) and various heavy metals, the sorptive properties and mechanisms of biodegradable MPs remain a notable knowledge gap. Given their different chemical compositions, surface functionalities, and physical structures (often more porous due to manufacturing or initial degradation), biodegradable MPs may interact with contaminants in fundamentally different ways, potentially posing distinct environmental risks that are not captured by extrapolating from data on conventional plastics.

Among the various toxic elements that co-occur with MPs in contaminated environments, arsenic (As) stands out due to its high toxicity, mobility, and prevalence. Arsenic, a ubiquitous metalloid element prevalent throughout the Earth's lithosphere, exhibits naturally occurring baseline levels in terrestrial soils that fluctuate considerably across geographical regions, typically averaging approximately 5–10 milligrams per kilogram. However, human-induced activities—including mineral extraction, metallurgical processing, industrial effluent discharge, and the legacy application of arsenic-containing agrochemicals—have precipitated significant contamination across numerous geographical areas. Within environmental matrices, arsenic manifests in various valence states, among which arsenite and arsenate represent the predominant inorganic species encountered in aquatic systems and terrestrial environments. Under oxidizing conditions, arsenate typically prevails as the principal species, and due to its structural resemblance to phosphate, it can be readily assimilated by vegetation via phosphate uptake pathways. Human exposure to arsenic-tainted dietary sources and potable water has been associated with numerous deleterious health outcomes, notably dermatological manifestations such as skin lesions, as well as cardiovascular pathologies, neurodegenerative conditions, and multiple malignancies. The biogeochemical circulation of arsenic is intricate, governed by redox potential, hydrogen ion concentration, and the availability of mineral interfaces and organic constituents. The introduction of a new, pervasive particulate phase like MPs adds another layer of complexity to this cycle.

Preliminary studies have confirmed that MPs can indeed adsorb arsenic. For example, research has shown that PE-MPs and PS-MPs can remove As from aqueous solutions through mechanisms believed to involve electrostatic attraction and surface complexation [19, 20]. However, these studies have predominantly focused on a limited set of traditional polymers. The adsorption capacity, kinetics, affinity, and underlying molecular-scale mechanisms are likely highly dependent on the physicochemical properties of the MP. Critical determinants encompass specific surface area, pore structure characteristics, and surface electrostatic properties (quantified as the point of zero charge), along with the abundance and chemical nature of surface functional moieties,

including carbonyl (C=O), ester (C-O-C), hydroxyl (-OH), and non-polar hydrocarbon (C-H) groups. Biodegradable polymers like PCL and PLA are polyester-based, meaning their backbone contains ester linkages and terminal or side-chain carbonyl groups. These oxygen-containing functional groups are potential sites for specific chemical interactions with arsenic oxyanions (e.g., H_2AsO_4^- , HAsO_4^{2-}) through mechanisms such as ligand exchange, hydrogen bonding, or inner-sphere complexation. In contrast, the surfaces of PE and PP are primarily composed of non-polar C-H bonds, limiting interactions largely to non-specific physical adsorption (e.g., van der Waals forces) or weak outer-sphere complexes. Furthermore, the degradation process of materials like PCL and PLA could dynamically alter their surface properties over time, potentially increasing porosity and exposing new functional groups, thereby changing their sorptive behavior in ways that static, non-degrading PE and PP would not.

The geographical context of this study is particularly relevant. The intensive use of plastic film mulching technology here is among the highest in the nation, with a covered area exceeding 35,000 km² [21]. This widespread application, coupled with challenges in complete film recovery, suggests that Xinjiang's soils may harbor significant loads of both conventional and, increasingly, biodegradable MPs. If these regions also have backgrounds or hotspots of arsenic contamination (from natural geological sources or historical activities), the potential for MP-As composite pollution is substantial. Understanding the nature of this interaction is therefore not merely an academic exercise but a pressing need for environmental risk assessment and the development of sustainable agricultural practices.

In light of the above, this study was designed to systematically compare and contrast the adsorption behaviors and mechanisms of As(V) onto conventional, Given these considerations, the present investigation was undertaken to rigorously evaluate and differentiate the As(V) sorption characteristics and underlying mechanisms between traditional non-biodegradable microplastics (polyethylene and polypropylene) and their biodegradable counterparts (polycaprolactone and polylactic acid). The following hypotheses were proposed: (1) elevated porosity, and abundance of polar surface functional groups; (2) the sorption kinetics of biodegradable microplastics will be markedly more rapid relative to conventional polymers, attributable to enhanced surface reactivity and accessibility of active binding sites; and (3) distinct mechanistic pathways will govern As(V) uptake between these two polymer categories, reflecting differences in surface chemistry and structural properties. (1) enhanced pore volume, and the prevalence of oxygen-rich polar functionalities on their surfaces. (2) The adsorption kinetics will be faster for biodegradable MPs and will be better described by a chemisorption-based model, whereas adsorption onto conventional MPs will be governed by a combination of physisorption and weak chemical interactions; (3) Particle size reduction will enhance adsorption for all MPs, but this effect will be more pronounced for conventional MPs whose adsorption is more critically dependent on external surface area. To test these hypotheses, we conducted comprehensive batch adsorption experiments investigating both adsorption isotherms and kinetics across three particle sizes (100, 150, and 200 μm). The collected experimental results were subjected to rigorous mathematical modeling, employing both Langmuir and Freundlich equilibrium isotherms alongside pseudo-first-order and pseudo-second-order kinetic rate equations. Additionally, comprehensive material characterization was conducted utilizing an array of sophisticated analytical methodologies, specifically Scanning Electron Microscopy coupled with Energy Dispersive X-ray Spectroscopy, Fourier Transform Infrared Spectroscopy, X-ray Diffraction, and X-ray Photoelectron Spectroscopy—to investigate morphological, structural, and chemical alterations occurring within the microplastic matrices subsequent to arsenate uptake. This multi-faceted approach allows us to move beyond empirical fitting parameters and elucidate the fundamental mechanisms driving the observed differences in adsorption behavior. The findings from this research will fill a critical gap in our understanding of the environmental behavior of biodegradable MPs and provide a vital scientific foundation for accurately assessing the composite pollution risks they may pose in conjunction with toxic metals like arsenic. Ultimately, this knowledge is essential for informing the development of rational, evidence-based environmental management policies and agricultural practices that balance productivity with long-term ecological health.

2 Materials and Methods

2.1 Test Materials

The test MPs were purchased from Dongguan Qianjing New Material Co., Ltd. Three particle sizes (100 μm , 150 μm , 200 μm) of polyethylene (PE), polypropylene (PP), polycaprolactone (PCL), and polylactide (PLA) were selected as the test MPs. Among them, PE-MPs and PP-MPs are non-degradable microplastics, while PCL-MPs and PLA-MPs are degradable microplastics. Prior to experimental use, the specimens underwent pre-treatment involving immersion in 0.1 mol·L⁻¹ hydrochloric acid solution for surface heavy metal elimination, followed by triple rinsing with deionized water and ambient temperature desiccation. The arsenate stock solution employed for preparing experimental solutions at varying As(V) concentrations was procured from the National Center for Nonferrous Metals and Electronic Materials Analysis and Testing. Arsenic(V) occurs as the arsenate anion, with the molecular formula AsO₄³⁻, at a mass concentration of 1000 micrograms per milliliter.

2.2 Adsorption Experiments

2.2.1 Isothermal Adsorption Experiment

1.0 g each of 100 μm PE-MPs, PP-MPs, PCL-MPs, and PLA-MPs were weighed separately. Then, 20 mL of As(V) solution with concentrations of 0.5, 1, 2, 4, 6, 8 mg·L⁻¹ was added. The mixtures were shaken in a constant temperature shaker at room temperature in the dark for 24 hours. After shaking, samples were taken to determine the mass concentration of As in the solution. Triplicate measurements were conducted for each specimen, with the arithmetic mean of the three replicate values adopted as the definitive result. The acquired equilibrium sorption data were subjected to nonlinear regression analysis employing the Langmuir [Equation (1)] and Freundlich [Equation (2)] mathematical models. Their expressions are respectively:

$$\frac{C_e}{q_e} = \frac{1}{b \cdot q_m} + \frac{C_e}{q_m} \quad (1)$$

$$\ln q_e = \ln K_f + \frac{1}{n} \ln C_e \quad (2)$$

Where, Q_e is the equilibrium adsorption capacity of MPs for As, mg·g⁻¹; C_e is the equilibrium concentration of As in the solution, mg·L⁻¹; K_f is the Freundlich distribution coefficient; n represents the nonlinear degree of the adsorption isotherm, dimensionless; Q_m is the theoretical maximum adsorption capacity, mg·g⁻¹; K_L is the Langmuir adsorption constant, L·mg⁻¹.

2.2.2 Adsorption Kinetics Experiment

Individual aliquots of 1.0 gram were precisely weighed for each microplastic type—specifically polyethylene, polypropylene, polycaprolactone, and polylactic acid particles—with a uniform particle diameter of 100 micrometers. Twenty milliliters of arsenate solution at a concentration of 0.5 milligrams per liter were introduced into each experimental group. The reaction mixtures were subjected to continuous agitation in a thermostated orbital shaker under ambient temperature conditions, with aliquots withdrawn at predetermined time intervals of 5, 10, 30, 60, 120, 240, 480, 960, and 1440 minutes to monitor the temporal evolution of adsorption. Following centrifugal separation, the resultant supernatant was passed through a 0.45 micrometer pore-size membrane filter and subsequently subjected to a hundred-fold dilution. The residual arsenic concentration in the processed solution was then quantified utilizing an atomic fluorescence spectrophotometer (Model PF-3, Beijing Puxi Instrument Co., Ltd.). Triplicate analyses were performed for every specimen with the mean value of the three replicate determinations adopted as the definitive outcome. The adsorption amount was calculated according to Formula (3):

$$q_t = \frac{(C_0 - C_t)m}{v} \quad (3)$$

Where: Q_t is the adsorption amount at time t , mg·kg⁻¹; C_t and C_0 are the concentrations of As(V) in the solution at time t and before adsorption, respectively, mg·L⁻¹; V is the volume of the As(V) solution, mL; m is the mass of the adsorbent, g.

The acquired kinetic data were subjected to nonlinear regression analysis employing the pseudo-first-order [Equation (4)] and pseudo-second-order [Equation (5)] rate equations. Their expressions are respectively:

$$\ln(q_e - q_t) = \ln q_e - k_1 t \quad (4)$$

$$\frac{t}{q_t} = \frac{1}{k_2 \cdot q_e^2} + \frac{t}{q_e} \quad (5)$$

Where: Q_e is the equilibrium adsorption capacity, $\text{mg}\cdot\text{g}^{-1}$; Q_t is the adsorption amount at time t , $\text{mg}\cdot\text{g}^{-1}$; K_1 is the rate constant of the pseudo-first-order adsorption reaction, min^{-1} ; K_2 is the rate constant of the pseudo-second-order adsorption reaction, $\text{g}\cdot(\text{mg}\cdot\text{min})^{-1}$.

2.2.3 Adsorption Kinetics Experiment of MPs with Different Particle Sizes

1.0 g each of 100 μm , 150 μm , 200 μm PE-MPs, PP-MPs, PCL-MPs, PLA-MPs were weighed separately. 20 mL of 0.5 $\text{mg}\cdot\text{L}^{-1}$ As(V) solution was added to each treatment group. The mixtures were placed in a constant temperature shaker for adsorption at room temperature, and samples were taken at 5, 10, 30, 60, 120, 240, 480, 960, 1440 min. The measurement steps were the same as the adsorption kinetics experiment.

2.3 Sample Characterization and Data Processing

Scanning electron microscopy was employed to examine the surface topographical features of the specimens. Fourier-transform infrared spectroscopy and X-ray diffraction were utilized to characterize the functional moieties, crystallographic structure, and surface elemental constituents of the materials. WPS 2025 was used for data statistics and analysis; R packages (ggplot2, dplyr, minpack.lm) and Origin 2022 were used for chart plotting and data analysis.

3 Results and Analysis

3.1 Differences in Pore Structure and Functional Groups between Traditional MPs and Degradable MPs

The pore structure parameters of 100 μm traditional MPs and degradable MPs are shown in Table 1. As presented in Table 1, polyethylene and polypropylene microplastics exhibit comparable specific surface areas and total pore volumes, whereas the biodegradable polycaprolactone and polylactic acid microplastics demonstrate similarly analogous specific surface areas and total pore volumes. Notably, the specific surface area of biodegradable microplastics is approximately five-fold greater than that of their non-biodegradable counterparts. Additionally, the total pore volume of biodegradable microplastics is roughly an order of magnitude higher compared to conventional non-degradable polymers. The average pore diameters of the four types of microplastics are similar.

Table 1 Pore structure parameters of 100 μm PE-MPs, PP-MPs, PCL-MPs, PLA-MPs

MPs Material	Specific Surface Area / $\text{m}^2\cdot\text{g}^{-1}$	Total Pore Volume / $\text{cm}^3\cdot\text{g}^{-1}$	Average Pore Diameter / nm
PE	7.32	0.0198	10.8
PP	7.92	0.0205	11.2
PCL	37.8	0.237	11.4
PLA	34.5	0.205	10.0

The SEM images of the four types of MPs are shown in Figure 1. There are significant differences in surface morphology between degradable MPs and non-degradable MPs. The surfaces of PE and PP are spherical, relatively smooth compared to PCL and PLA, with PE having more cracks. The surfaces of PCL and PLA are irregularly blocky, with PCL exhibiting fragmented textures.

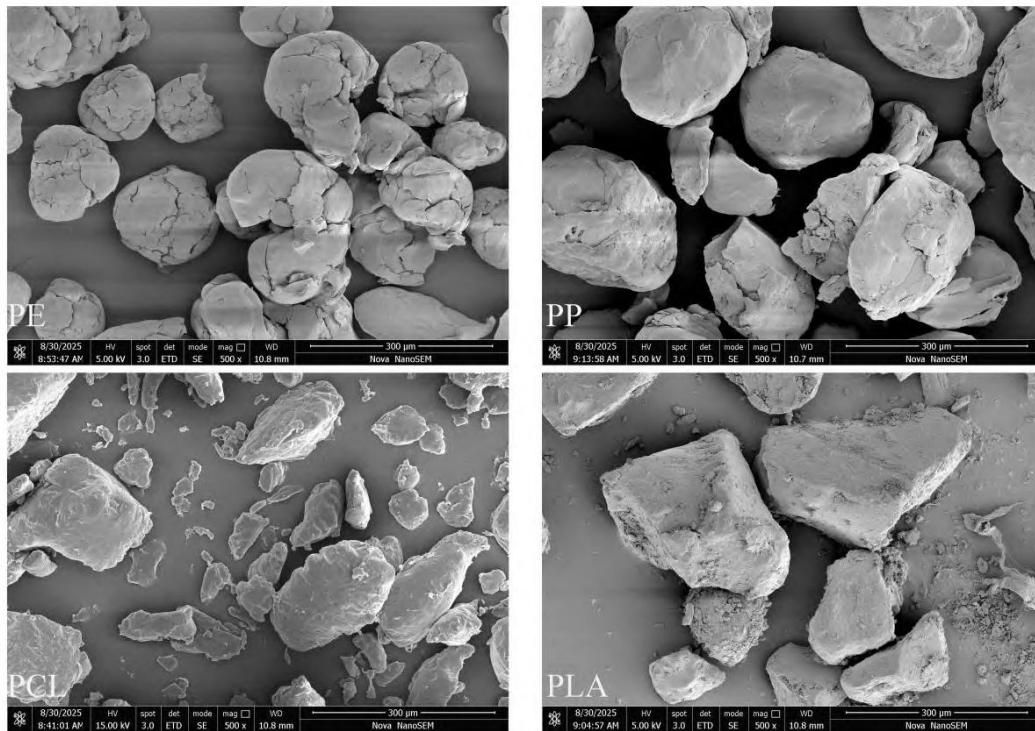


Figure 1 SEM-EDS images of different types of MPs

The FTIR spectra of the four types of MPs are shown in Figure 2. All four types of MPs have vibration peaks related to C-H bonds such as methylene $-CH_2-$ and methyl $-CH_3$ at $500-750\text{ cm}^{-1}$, $1250-1500\text{ cm}^{-1}$, and $2750-3000\text{ cm}^{-1}$. Degradable MPs PCL and PLA have vibration peaks related to C=O at $1500-1750\text{ cm}^{-1}$ and C-O-C at $1000-1250\text{ cm}^{-1}$ that constitute ester bonds, while non-degradable MPs PE and PP do not.

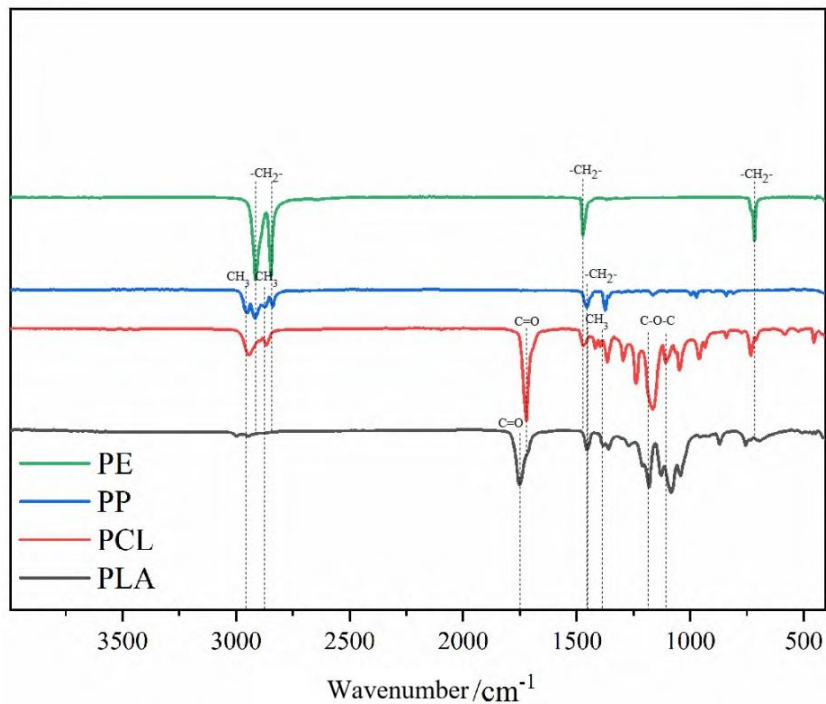


Figure 2 FTIR spectra of four types of MPs before adsorption As

3.2 Isothermal Adsorption Characteristics of As on Traditional MPs and Degradable MPs

The Langmuir and Freundlich adsorption isotherm fitting curves for arsenic onto the four microplastic types are illustrated in Figures 3(a) and 3(b), respectively, with the corresponding modeling parameters summarized in Table 2. The coefficient of determination (R^2) values for both Langmuir and Freundlich models applied to the arsenic adsorption isotherms across all four microplastic types exceeded 0.96, demonstrating that both theoretical frameworks adequately describe the sorption behavior of arsenate onto these polymer surfaces. The Langmuir isotherm exhibited superior goodness-of-fit relative to the Freundlich model for arsenate sorption onto all four microplastic variants, suggesting that arsenic uptake on microplastic surfaces predominantly follows monolayer coverage characteristics.

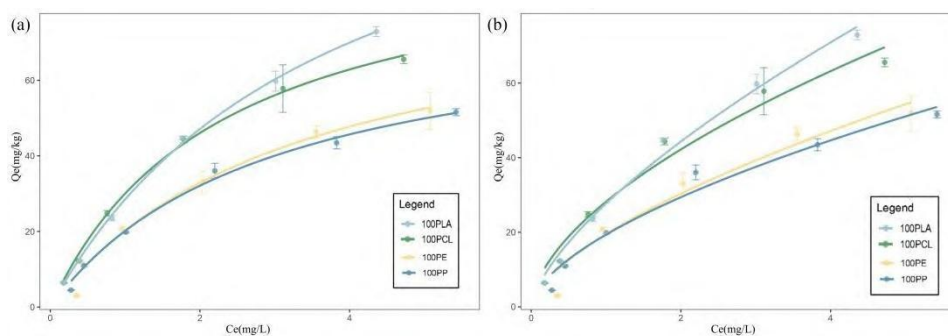


Figure 3 Adsorption isotherms of As on different types of MPs

Table 2 Parameters of Langmuir and Freundlich isotherm adsorption models for As on different types of MPs

Plastic Type	Langmuir Model			Freundlich Model		
	KL(L·mg ⁻¹)	qm(mg·kg ⁻¹)	R2	KF(mg ¹⁻ⁿ ·L·g ⁻¹)	n	R2
PE	0.30	87.18	0.981	19.50	1.37	0.961
PP	0.34	79.12	0.993	19.36	1.56	0.972
PCL	0.44	98.94	0.998	28.20	1.72	0.972
PLA	0.27	135.93	0.999	27.70	1.68	0.991

The model fitting parameters show that the adsorption capacities of the four MPs are ranked from largest to smallest as: PLA-MPs (135.93 mg·kg⁻¹) > PCL (98.94 mg·kg⁻¹) > PE (87.18 mg·kg⁻¹) > PP (79.12 mg·kg⁻¹). The adsorption capacities of the two degradable MPs are greater than those of the two non-degradable MPs. The adsorption capacity of PLA-MPs is 71.8% higher than that of PP-MPs. The Freundlich model parameter n value represents the strength of interaction between MPs and As. The n values for the four MPs, from largest to smallest, are: PCL (1.72) > PLA (1.68) > PP (1.56) > PE (1.37), indicating that the adsorption strength of degradable MPs for As is greater than that of non-degradable MPs.

3.3 Adsorption Kinetic Characteristics of As on Traditional MPs and Degradable MPs

The temporal adsorption data for arsenic onto the four microplastic types were subjected to kinetic modeling using both pseudo-first-order and pseudo-second-order rate equations. The resultant kinetic fitting curves are presented in Figures 4(a) and 4(b), with the corresponding model parameters detailed in Table 3. The modeling outcomes demonstrate that both the pseudo-first-order and pseudo-second-order kinetic frameworks adequately capture the arsenic adsorption behavior on microplastic surfaces. The coefficients of determination for pseudo-first-order and pseudo-second-order kinetics applied to arsenic sorption on conventional microplastics were comparable, suggesting that the underlying sorption mechanisms cannot be exclusively attributed to either physical diffusion or chemisorption processes alone, but rather arises from the synergistic interplay of multiple concurrent interaction mechanisms. Conversely, the coefficient of determination for pseudo-second-order kinetics exceeded that of the pseudo-first-order model when applied to arsenic sorption on biodegradable microplastics, indicating that while both physisorption and chemisorption contribute to arsenic uptake on biodegradable microplastics, the latter mechanism predominates.

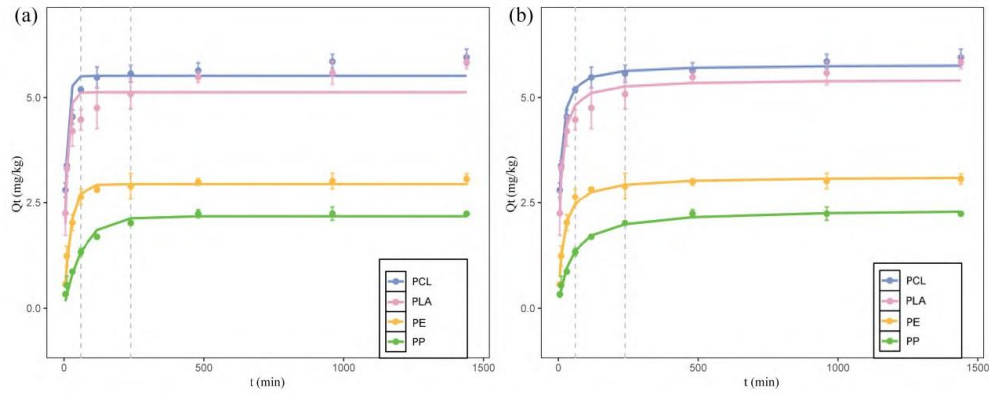


Figure 4 Adsorption kinetic curves of As on four types of MPs

As shown in the figure, the overall trends of the four MPs are consistent. The adsorption kinetic process can be roughly divided into a rapid adsorption stage (0~60 min), a slow adsorption stage (60~240 min), and an adsorption equilibrium stage (240~1440 min). In the rapid adsorption stage, the adsorption rate of MPs for As is the fastest.

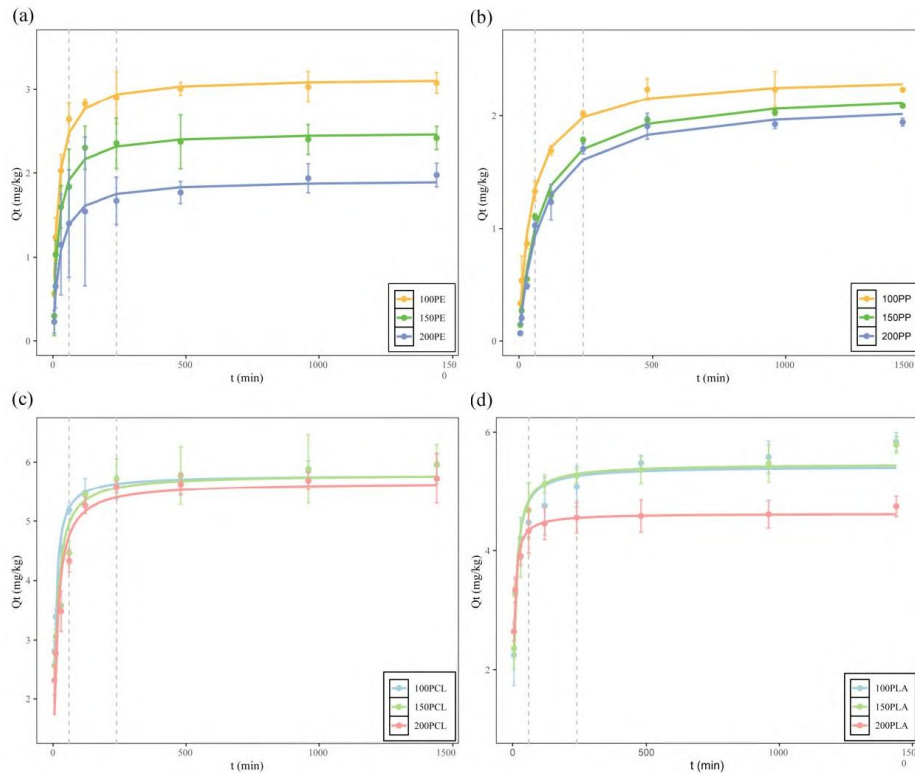


Figure 5 Adsorption kinetic curves of As on three particle sizes of PE-MPs、PP-MPs、PCL-MPs、PLA-MPs

This is because there are more adsorption sites on the MP surfaces and the As concentration in the reaction system is higher in the initial stage of adsorption. During the deceleration phase, as available binding sites on the microplastic surfaces become progressively saturated with arsenate ions, the overall sorption rate diminishes accordingly. When the reaction enters the adsorption equilibrium stage, the adsorption of As by MPs gradually tends to equilibrium. At this time, as the adsorption reaction proceeds, the adsorption sites in the MPs are further occupied, and the As concentration in the solution further decreases compared to the slow adsorption stage. Finally, the adsorption reaction reaches an equilibrium state. The slope of the adsorption curve can indicate the magnitude of the adsorption rate. It can be seen from the figure that PCL has the largest slope,

followed by PLA, and PP has the smallest slope. Therefore, the adsorption rates of the four MPs for As are: PCL-MPs > PLA-MPs > PE-MPs > PP-MPs. The adsorption rates of degradable microplastics are higher than those of non-degradable microplastics at all stages. The larger the adsorption rate constant K_2 , the faster the adsorption rate and the stronger the chemical interaction. The adsorption rate constants K_2 for the four MPs are: PCL-MPs > PLA-MPs > PE-MPs > PP-MPs, indicating that the adsorption rate and strength of degradable MPs for As are higher than those of non-degradable MPs.

Table 3 Fitting parameters of pseudo-first-order and pseudo-second-order kinetic models for the adsorption of As on four types of MPs

Plastic Type	Pseudo-first-order Model			Pseudo-second-order Model		
	$q_e(\text{mg}\cdot\text{kg}^{-1})$	$k_1(\text{min}^{-1})$	R^2	$q_e(\text{mg}\cdot\text{kg}^{-1})$	$k_2(\text{g}\cdot\text{mg}^{-1}\cdot\text{min}^{-1})$	R^2
PE	2.95	0.043	0.984	3.13	0.020	0.989
PP	2.18	0.016	0.972	2.35	0.010	0.992
PCL	5.51	0.105	0.870	5.78	0.027	0.980
PLA	5.13	0.099	0.825	5.43	0.025	0.944

3.4 Effect of Particle Size on As Adsorption by MPs

The temporal sorption data for arsenic onto the four microplastic variants across three distinct particle size fractions (100, 150, and 200 micrometers) were modeled using the pseudo-second-order kinetic equation. The resultant kinetic fitting curves are illustrated in Figures 5(a) through 5(d), with the corresponding model parameters summarized in Table 4. The equilibrium adsorption capacities of the three MPs at 100 μm particle size are greater than those at 150 μm and 200 μm particle sizes, indicating stronger adsorption capacity. Overall, in terms of both equilibrium rate and concentration, degradable MPs are greater than non-degradable MPs. The influence of particle dimensions on sorption behavior is more pronounced for conventional non-biodegradable microplastics compared to their biodegradable counterparts. Among the polymers examined, polyethylene microplastics exhibited the most substantial response to variations in particle size. As the particle size increases from 100 μm to 200 μm , its adsorption capacity decreases by 38.7%.

Table 4 Fitting parameters of pseudo-second-order kinetic models for the adsorption of As on three particle sizes of PE-MPs, PP-MPs, PCL-MPs, PLA-MPs

Plastic Type	Pseudo-second-order Model		
	$q_e(\text{mg}\cdot\text{kg}^{-1})$	$k_2(\text{g}\cdot\text{mg}^{-1}\cdot\text{min}^{-1})$	R^2
100 μm PE	3.13	0.020	0.989
150 μm PE	2.49	0.023	0.975
200 μm PE	1.92	0.023	0.982
100 μm PP	2.35	0.010	0.992
150 μm PP	2.22	0.006	0.992
200 μm PP	2.12	0.006	0.989
100 μm PCL	5.78	0.027	0.980
150 μm PCL	5.79	0.017	0.903
200 μm PCL	5.66	0.016	0.932
100 μm PLA	4.62	0.055	0.987
150 μm PLA	5.47	0.024	0.960
200 μm PLA	5.43	0.024	0.944

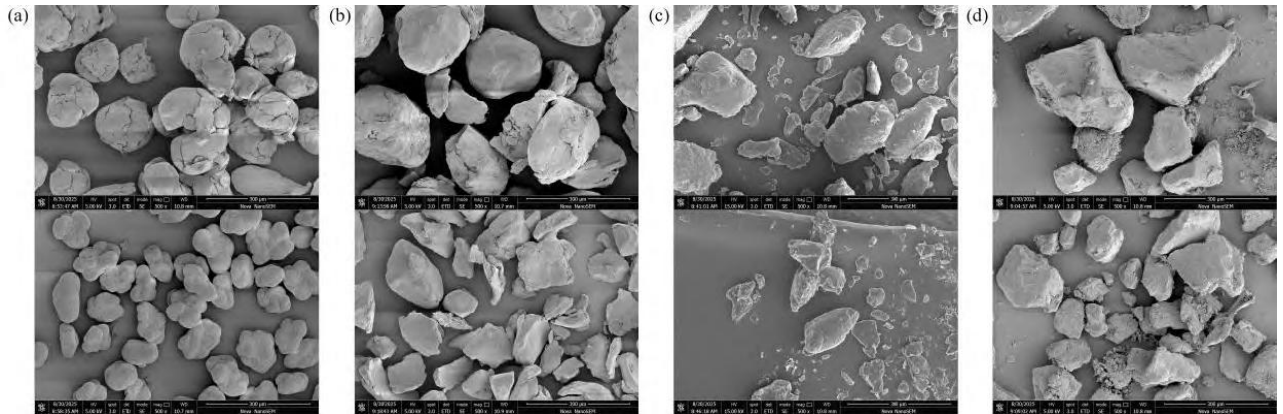


Figure 6 SEM-EDS images of soils different types of MPs before and after adsorption of As

3.5 Characterization of Four Types of MPs Before and After As Adsorption

The SEM-EDS images of the four types of MPs before and after As adsorption are shown in Figure 6(a~d). After As adsorption, PE (a) overall presents an irregular near-spherical or aggregated particle shape, with slight depressions formed in local areas. It had irregular cracks before adsorption and became smoother after adsorption. PP (b) shows an irregular blocky or flaky structure after As adsorption, with distinct edges and a relatively dense surface. The particles are more tightly bonded, but minor cracks and layered peeling are also visible. Both PCL (c) and PLA (d) exhibit relatively obvious brittle fracture characteristics, appearing as irregular solid fragments with sharp and distinct edges and corners. In contrast, their surfaces are relatively smooth and flat, with relatively few pore structures.

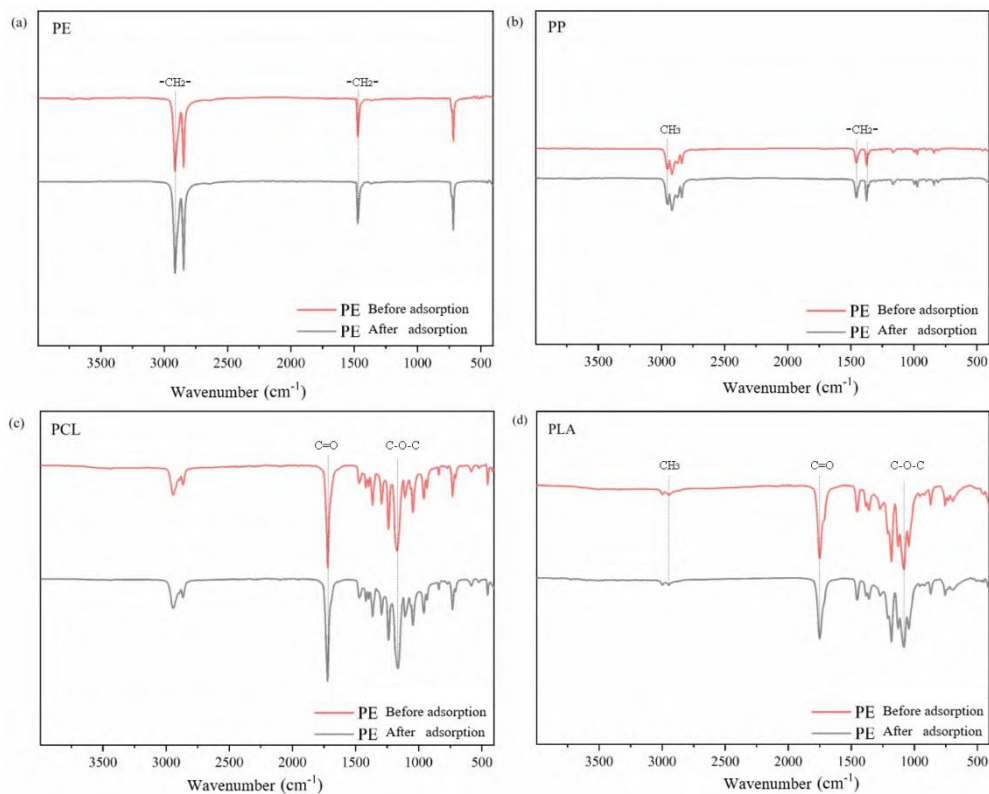


Figure 7 SFTIR spectra of PE-MPs, PP-MPs, PCL-MPs and PLA-MPs before and after adsorption As

Fourier-transform infrared spectroscopy was employed to investigate alterations in surface functional group

chemistry for all four microplastic types prior to and following arsenate uptake. The findings are presented graphically in Figures 7(a) through 7(d). No new peaks appeared in the four MPs after As adsorption, but the peak areas all decreased to a certain extent, indicating that some functional groups were consumed during the adsorption process to bind with As. After As adsorption on PE, the peak areas of $\text{-CH}_2\text{-}$ at 1500 cm^{-1} and $2750\text{-}3000\text{ cm}^{-1}$ decreased. After As adsorption on PP, the peak areas of $\text{-CH}_2\text{-}$ and -CH_3 at $1250\text{-}1500\text{ cm}^{-1}$ and $2750\text{-}3000\text{ cm}^{-1}$ decreased, indicating that the C-H groups in PE and PP may interact with As through C-H bonds, serving as adsorption sites for As. After As adsorption on PCL and PLA, the peak areas of C=O at $1500\text{-}1750\text{ cm}^{-1}$ and C-O-C at $1000\text{-}1250\text{ cm}^{-1}$ decreased, indicating that ester-related groups such as C=O and C-O-C in degradable MPs are the main adsorption sites. PCL and PLA also showed slight fluctuations in the methylene $\text{-CH}_2\text{-}$ and -CH_3 peaks at $2750\text{-}3000\text{ cm}^{-1}$, proving that C-H bonds also participated in the As adsorption process by degradable MPs.

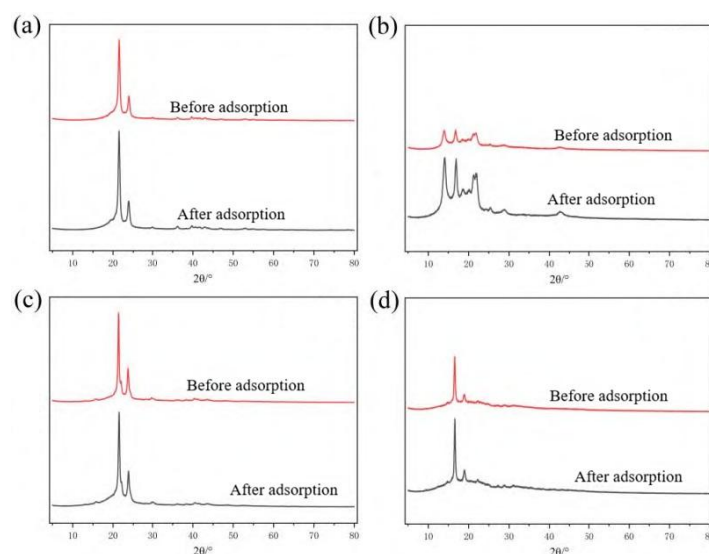


Figure 8 XRD spectra of PE-MPs, PP-MPs, PCL-MPs and PLA-MPs before and after adsorption As

XRD spectroscopy can further analyze the existing forms of As on the MP surfaces after the reaction. Figure 8 shows the XRD spectra of the four MPs before and after As adsorption. A reduction in the integrated area of crystalline diffraction peaks signifies diminished crystalline order within the polymer matrices, indicating that chemical transformations took place throughout the sorption process, thereby compromising the structural integrity of the microplastic surface lattice. After adsorption, the characteristic crystalline peaks of the four MPs did not shift, and no significant new peaks were generated. The crystalline peak areas of PE, PCL, and PLA slightly decreased, while the crystalline peak area of PP significantly decreased. This indicates that the PP structure is more sensitive. During the adsorption reaction process, the reaction between PP and As is concentrated in the crystalline region, while the reactions between the other three MPs and As are concentrated in the amorphous region. Although the damage to PP is the most significant, its adsorption capacity is still lower than the other three MPs. The reason may be that PP contains -CH_3 compared to PE, which increases the chain spacing and hinders PP adsorption. PCL and PLA contain strong adsorption sites like C=O and C-O-C, and have a larger specific surface area, leading to their higher adsorption capacity than PE and PP.

XPS spectroscopy can further analyze the existing forms of As on the MP surfaces after the reaction. Figure 9 shows the XPS spectra of the four MPs after As adsorption. The results show that characteristic peaks of As appear in all four MPs after As adsorption, indicating that all four MPs adsorbed As. Peak fitting of the As 3d high-resolution spectra revealed the presence of characteristic peaks for As(III), indicating that electron transfer occurred during the adsorption process, and part of As(V) was reduced to As(III). As combines with the MP surface by gaining electrons. Furthermore, the proportion of As(III) is relatively higher in degradable MPs, suggesting that oxygen-containing functional groups (C=O, C-O-C) may coordinate with As(V), leading to its reduction.

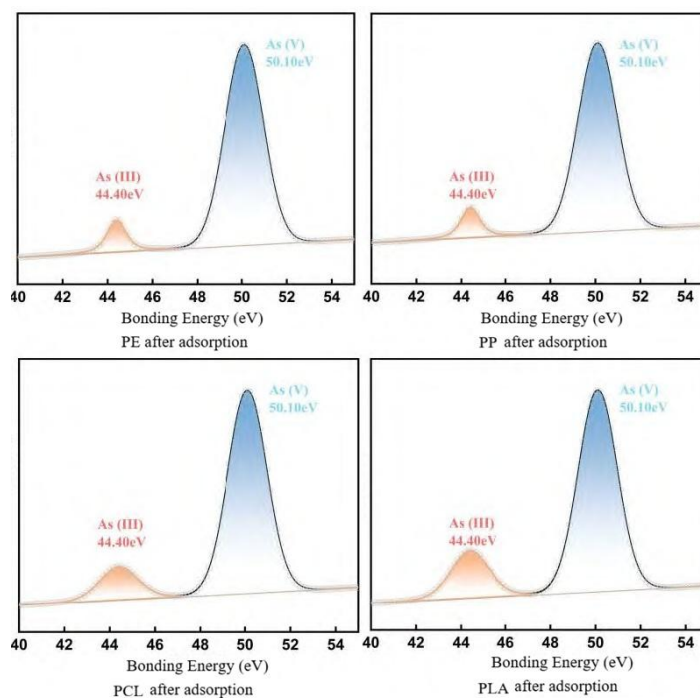


Figure 9 XPS spectra of PE-MPs, PP-MPs, PCL-MPs and PLA-MPs after adsorption As

4 Discussion

Guo and colleagues [23] demonstrated that specific surface area serves as a critical determinant governing cadmium sorption onto microplastic particles. Similarly, Gao et al. [24] established a correlation between heavy metal uptake efficiency and the dimensional characteristics of plastic particulates. In this study, the specific surface area of 100 μm degradable MPs is about 5 times that of traditional MPs, and the total pore volume is about 10 times. A larger specific surface area means more exposed potential adsorption sites, and the developed pore structure provides channels for the diffusion of As(V) ions into the particle interior, thereby significantly improving adsorption mass transfer efficiency and rate. The adsorption capacity of traditional MPs significantly increases with decreasing particle size (i.e., increasing specific surface area), especially for PE, indicating that their adsorption relies more on the external surface. In contrast, degradable MPs, due to their inherent developed internal pores, are less sensitive to particle size changes, indicating that their porous structure can maintain high adsorption performance even at larger particle sizes.

The outcomes of this investigation furnish an exhaustive, mechanism-oriented elucidation of the divergent sorption characteristics exhibited by arsenate on traditional versus biodegradable microplastic materials. The superior adsorption performance of biodegradable MPs (PCL and PLA) over their conventional counterparts (PE and PP) is not a singular phenomenon but the result of a synergistic interplay of several interconnected physicochemical factors, primarily their structural morphology, surface chemistry, and the consequent adsorption mechanisms. This discussion will delve into these factors, contextualize our findings within the broader literature, and explore the nuanced environmental implications of these differences.

1. The Fundamental Role of Physicochemical Properties: Morphology, Porosity, and Surface Functionality

The stark contrast in specific surface area (SSA) and total pore volume between the two MP types is the foundational physical determinant of their differential adsorption capacities. Our measurements show that PCL and PLA possess SSAs approximately 5 times greater and pore volumes about 10 times larger than those of PE and PP. This aligns with the SEM observations, where PCL and PLA exhibited irregular, fragmented, and textured surfaces, while PE and PP appeared more smooth and spherical. A higher SSA directly translates to a greater number of potential adsorption sites being exposed to the aqueous phase. More importantly, the significantly

larger pore volume, particularly in the mesoporous range as suggested by the average pore diameters (~10-11 nm), facilitates the intraparticle diffusion of As(V) oxyanions (e.g., H_2AsO_4^- , HAsO_4^{2-}) into the internal pore structure of the biodegradable MPs. This creates a three-dimensional adsorption matrix rather than reliance solely on external surface sites. The work of Guo et al. [23] on Cd adsorption highlighted SSA as a critical factor, a principle strongly corroborated here. The internal porosity of PCL and PLA means that even as external sites are occupied, the concentration gradient can drive further As(V) into the particle interior, supporting a higher equilibrium capacity (Q_m). In contrast, the adsorption on PE and PP is largely confined to their limited external surface, leading to quicker site saturation and lower maximum capacities.

Beyond physical structure, surface chemistry dictates the affinity and strength of the interaction. FTIR analysis conclusively identified the key functional groups. The surfaces of PCL and PLA are rich in polar, oxygen-containing functional groups, chiefly the carbonyl (C=O) and ether (C-O-C) groups inherent to their polyester structures. These groups are not merely spectators; they are active participants in adsorption. The pronounced attenuation in the intensities of carbonyl (C=O) and ester (C-O-C) stretching bands observed in the post-adsorption FTIR spectra offers direct spectroscopic confirmation that these oxygen-containing functionalities serve as the principal loci for arsenate binding. The oxygen atoms within these functional groups bear non-bonding electron pairs, conferring upon them the capacity to function as Lewis base sites. They can form specific chemical bonds with As(V) species through mechanisms such as ligand exchange (where a hydroxyl group on the arsenate anion replaces a weaker ligand on the MP surface) or the formation of inner-sphere complexes via coordination bonding. This is a strong, specific, and often irreversible form of chemisorption. Conversely, the surfaces of PE and PP are dominated by non-polar aliphatic C-H and $-\text{CH}_2/\text{CH}_3$ groups. These groups can only interact with As(V) anions through much weaker, non-specific forces such as van der Waals interactions or possibly very weak hydrogen bonding with minimal charge separation. The observed minor decrease in C-H peak intensities post-adsorption suggests such weak physical adsorption occurs, but it lacks the directional strength and specificity of the chemical interactions seen with biodegradable MPs.

2. Kinetic and Isotherm Analysis: Deciphering the Dominant Mechanisms

The modeling of adsorption kinetics and isotherms provides a quantitative framework that supports the mechanistic insights from characterization. The adsorption isotherms for all four MPs were well-described by both Langmuir and Freundlich models, but the consistently higher R^2 values for the Langmuir model suggest a trend toward monolayer coverage on relatively homogeneous sites. The Langmuir maximum adsorption capacity (q_m) followed the order $\text{PLA} > \text{PCL} > \text{PE} > \text{PP}$, perfectly correlating with the trend in SSA and the presence of oxygen functional groups. The Freundlich parameter n , an indicator of adsorption intensity or surface heterogeneity, was greater for PCL (1.72) and PLA (1.68) than for PP (1.56) and PE (1.37). An n value > 1 indicates favorable adsorption, and the higher values for biodegradable MPs confirm a stronger, more favorable interaction between their surfaces and As(V), consistent with chemisorption.

The kinetic analysis offers perhaps the clearest distinction. For biodegradable microplastics, the pseudo-second-order kinetic equation yielded substantially superior correlation coefficients compared to the pseudo-first-order model, indicating a pronouncedly better goodness-of-fit. The pseudo-second-order kinetic framework presupposes that the rate-determining step constitutes a chemisorption mechanism mediated by valence interactions, specifically electron sharing or exchange between adsorbent and adsorbate. The excellent fit to this model for PCL and PLA strongly indicates that their adsorption is rate-limited by surface chemical reaction at the C=O/C-O-C sites. In contrast, for conventional MPs (PE and PP), the R^2 values for the PFO and PSO models were very similar and both high. The PFO model typically describes diffusion-controlled processes. The comparable fit of both models suggests that the adsorption onto PE and PP lacks a single dominant rate-controlling step. Instead, it is likely a mixed process governed initially by boundary layer or film diffusion (a physical process) and later by weak surface interactions, with neither pure diffusion nor strong chemical reaction being exclusively rate-limiting. This mechanistic dichotomy—strong chemisorption vs. mixed weak physisorption—explains not only the higher capacity but also the generally faster initial adsorption rates observed for PCL and PLA (as indicated by their higher k_2 values).

3. The Differential Impact of Particle Size: Reinforcing the Mechanism Argument

The experiment with three particle sizes (100, 150, 200 μm) provided further compelling evidence for the differing adsorption mechanisms. Reducing particle size increases the specific surface area for all materials. We observed that this increase boosted adsorption for all MP types, but the effect was dramatically more pronounced for conventional MPs. For PE, the adsorption capacity dropped by 38.7% as particle size increased from 100 to 200 μm . This profound sensitivity indicates that adsorption onto PE and PP is critically dependent on external surface area. With few internal pores, the only way to expose more "sites" (even if weak) is to make the particles smaller.

In stark contrast, the adsorption capacity of PCL and PLA was much less affected by particle size changes. For PCL, the q_e values were nearly identical across all three sizes. This robustness indicates that their adsorption is not primarily surface-area-limited in this size range. Their highly porous, "sponge-like" structure means that even a larger particle (200 μm) still possesses a vast internal network of pores and channels accessible to As(V) ions. The total number of internal C=O/C-O-C sites remains high regardless of the overall particle dimension. This finding has significant environmental implications: even larger fragments of biodegradable plastics, which might be more mobile or ingested by different organisms, can still act as potent carriers for As, whereas the carrier potential of conventional MPs diminishes rapidly as their size increases.

4. Molecular-Level Insights from XPS and the Redox Transformation

The XPS analysis delivered a crucial, deeper layer of mechanistic understanding. The mere detection of an As signal confirmed adsorption. However, the deconvolution of the As 3d peak revealing the presence of both As(V) and As(III) was a pivotal finding. This indicates that a surface-mediated redox reaction occurred during adsorption. Part of the adsorbed As(V) was reduced to As(III) on the MP surfaces. This electron transfer process is a hallmark of a strong chemical interaction that goes beyond simple electrostatic attraction or physical entrapment.

The reason this is more pronounced for biodegradable MPs can be linked to their functional groups. The carbonyl group (C=O) is a potential electron donor. The oxygen atoms in the ester linkages (C-O-C) may also participate in electron transfer processes. We propose a potential mechanism: As(V) in the form of H_2AsO_4^- or HAsO_4^{2-} approaches the electron-rich oxygen of a C=O group. Through a coordination or ligand exchange process, an electron could be transferred from the MP's organic matrix to the arsenic center, reducing As(V) to As(III). This process would simultaneously stabilize the arsenic on the surface through the formation of a strong inner-sphere complex. The generated As(III) might then be retained or could potentially desorb, which has different toxicity and mobility implications. For traditional MPs, with their inert C-H bonds lacking readily donatable electrons, such a reduction process is far less likely, consistent with the weaker physical adsorption mechanism. This redox activity positions biodegradable MPs not just as passive carriers, but as potentially chemically active participants in the biogeochemical cycling of arsenic, potentially altering its speciation, toxicity, and mobility in the environment..

5 Conclusion

(1) The specific surface area of 100 μm degradable MPs (PCL, PLA) is about 5 times that of traditional MPs (PE, PP), and the total pore volume is about 10 times. Degradable MPs are rich in oxygen-containing polar groups such as C=O and C-O-C, while the surfaces of traditional MPs are mainly composed of non-polar groups such as C-H and -CH₂.

(2) The adsorption capacities of the four MPs for As(V) are in the order: PLA-MPs (135.93 $\text{mg}\cdot\text{kg}^{-1}$) > PCL-MPs (98.94 $\text{mg}\cdot\text{kg}^{-1}$) > PE-MPs (87.18 $\text{mg}\cdot\text{kg}^{-1}$) > PP-MPs (79.12 $\text{mg}\cdot\text{kg}^{-1}$). For conventional microplastics, the pseudo-first-order and pseudo-second-order kinetic models exhibited comparable degrees of goodness-of-fit, suggesting that the underlying sorption mechanisms are concurrently governed by physical mass transfer processes and relatively weak surface chemical interactions. Conversely, biodegradable microplastics demonstrated superior conformity to the pseudo-second-order kinetic framework, signifying that chemisorption constitutes the prevailing uptake mechanism. Biodegradable microplastics exhibit substantially enhanced sorption capacities and markedly accelerated uptake kinetics for arsenate compared to their conventional counterparts. (3) The adsorption capacities of the four MPs at 100 μm particle size are higher than those at 150

μm and $200\ \mu\text{m}$ particle sizes. The effect of particle size change on the adsorption performance of traditional MPs (especially PE-MPs) is significantly greater than that on degradable MPs, indicating that the adsorption of traditional MPs relies more on changes in specific surface area.

(4) The high adsorption performance of degradable MPs for As(V) stems from the abundant adsorption sites provided by their porous structure, and the strong chemical adsorption, mainly coordination, between the surface oxygen-containing functional groups (C=O, C-O-C) and As(V). In contrast, traditional MPs can only undergo weak physical adsorption with As(V) through non-polar groups such as C-H, resulting in lower adsorption capacity and binding strength.

References

- [1] Barbosa F, Adeyemi J A, Bocato M Z, et al. A critical viewpoint on current issues, limitations, and future research needs on micro- and nanoplastic studies: From the detection to the toxicological assessment [J]. *Environmental Research*, 2020, 182: 109089.
- [2] Thompson R C, Olsen Y, Mitchell R P, et al. Lost at sea: Where is all the plastic? [J]. *Science*, 2004, 304(5672): 838.
- [3] Liu M, Lu S, Song Y, et al. Microplastic and mesoplastic pollution in farmland soils in suburbs of Shanghai, China [J]. *Environmental Pollution*, 2018, 242: 855-862.
- [4] Scheurer M, Bigalke M. Microplastics in Swiss floodplain soils [J]. *Environmental Science & Technology*, 2018, 52(6): 3591-3598.
- [5] Wong J K H, Lee K K, Tang K H D, et al. Microplastics in the freshwater and terrestrial environments: Prevalence, fates, impacts and sustainable solutions [J]. *Science of The Total Environment*, 2020, 719: 137512.
- [6] Barnes D K A, Galgani F, Thompson R C, et al. Accumulation and fragmentation of plastic debris in global environments [J]. *Philosophical Transactions of the Royal Society B: Biological Sciences*, 2009, 364(1526): 1985-1998.
- [7] Prata J C. Airborne microplastics: Consequences to human health? [J]. *Environmental Pollution*, 2018, 234: 115-126.
- [8] Amato-Lourenço L F, dos Santos Galvão L, de Weger L A, et al. An emerging class of air pollutants: Potential effects of microplastics to respiratory human health? [J]. *Science of The Total Environment*, 2020, 749: 141676.
- [9] van Sebille E, Wilcox C, Lebreton L, et al. A global inventory of small floating plastic debris [J]. *Environmental Research Letters*, 2015, 10(12): 124006.
- [10] Blasing M, Amelung W. Plastics in soil: analytical methods and possible sources [J]. *Science of the Total Environment*, 2018, 612: 422-435.
- [11] Hu Jiani. Study on Pollution Characteristics of Microplastics in Farmland Soil and Environmental Behavior of Typical Plastic Film [D]. Shanghai: East China Normal University, 2021. DOI:10.27149/d.cnki.ghdsu.2021.000984.
- [12] Rillig M C. Microplastic in terrestrial ecosystems and the soil? [J]. *Environmental Science & Technology*, 2012, 46(12): 6453-6454.
- [13] Smedley P L, Kinniburgh D G. A review of the source, behaviour and distribution of arsenic in natural waters [J]. *Applied Geochemistry*, 2002, 17(5): 517-568.
- [14] Basu A, Saha D, Saha R, et al. A review on sources, toxicity and remediation technologies for removing arsenic from drinking water [J]. *Research on Chemical Intermediates*, 2014, 40(2): 447-485.
- [15] Shakoob M B, Nawaz R, Hussain F, et al. Human health implications, risk assessment and remediation of As-contaminated water: A critical review [J]. *Science of The Total Environment*, 2017, 601-602: 756-769.
- [16] Rehman M U, Khan R, Khan A, et al. Fate of arsenic in living systems: Implications for sustainable and safe food chains [J]. *Journal of Hazardous Materials*, 2021, 417: 126050.
- [17] Lange C N, Pedron T, Freire B M, et al. Arsenic in Rice Grain. In *The Future of Rice Demand: Quality Beyond Productivity* [M]. Springer International Publishing, 2020: 71-91.
- [18] Sadiq M. Arsenic chemistry in soils: an overview of thermodynamic predictions and field observations [J]. *Water, Air, and Soil Pollution*, 1997, 93(1): 117-136.
- [19] Sun Peipei. Interaction behaviors and mechanism between microplastics and arsenic [D]. Shanghai: East

China Normal University, 2022.

- [20] Dong Y, Gao M, Song Z, et al. As(III) adsorption onto different-sized polystyrene microplastic particles and its mechanism [J]. *Chemosphere*, 2020, 239: 124792.
- [21] Liu Ling, Chen Yulan. Current Situation, Problems and Control Measures of Agricultural Mulch Film Use in Xinjiang [J]. *Journal of Hebei Agricultural Sciences*, 2023, 27(04): 102-104.
- [22] Guo X, Liu Y, Wang J. Sorption of sulfamethazine onto different types of microplastics: a combined experimental and molecular dynamics simulation study [J]. *Marine Pollution Bulletin*, 2019, 145: 547-554.
- [23] Guo X, Hu G, Fan X, et al. Sorption properties of cadmium on microplastics: The common practice experiment and a two-dimensional correlation spectroscopic study [J]. *Ecotoxicology and Environmental Safety*, 2020, 190: 110118.
- [24] Gao F, Li J, Sun C, et al. Study on the capability and characteristics of heavy metals enriched on microplastics in marine environment [J]. *Marine Pollution Bulletin*, 2019, 144: 61-67.